The lattice strains in a specimen (cubic system) compressed nonhydrostatically in an opposed anvil device

Anil K. Singh
Materials Science Division, National Aeronautical Laboratory, Bangalore 560 017, India

(Received 21 September 1992; accepted for publication 1 January 1993)

A general expression has been derived using anisotropic elasticity theory for the lattice strain which corresponds to the x-ray diffraction measurement on the polycrystalline specimen (cubic system) compressed nonhydrostatically in an opposed anvil device. The expressions for the various diffraction geometries emerge as the special cases of this equation. The strain calculated using isotropic elasticity theory corresponds to the macroscopic strain in the specimen, and can be obtained from the present equation by letting the anisotropy factor $2(S_{11}-S_{12})/S_{44}=1$. Further, it is shown that the ratio of the lattice strain to the macroscopic strain (in the direction of the lattice strain) produced by the deviatoric stress component depends on the Miller indices (hkl) of the lattice planes and the elastic anisotropy factor. This ratio is unity only if the crystallites constituting the specimen are elastically isotropic, and increases with increasing anisotropy of the crystallites.

I. INTRODUCTION

The stress state in a solid specimen compressed between two flat and parallel anvil faces is nonhydrostatic.[1] The resulting lattice strains[6] measured by x-ray diffraction exhibit certain features which are absent if a truly hydrostatic condition prevails. In the past, two distinct approaches were used to theoretically analyze the situation. In the first approach,[7–9] anisotropic elasticity theory (AET) was used to derive the expression for the lattice strain in a cubic system, produced by nonhydrostatic stress. The analysis predicts that the measured lattice strain should depend on the Miller indices (hkl) of the set of planes used. This prediction was subsequently verified in a number of independent investigations.[7,10–16] In the second approach, isotropic elasticity theory (IET) was used to calculate the strain produced by nonhydrostatic pressure.[17–24] The two approaches have remained apparently distinct in the literature, with no attempts made for an intercomparison.

The earlier treatment of the subject had the drawback that each diffraction geometry was treated separately. In this article, a general expression has been derived using AET for the lattice strain produced by nonhydrostatic pressure. The expressions for the different diffraction geometries used in the high pressure work emerge as the special cases of this equation. The equations derived in the past using IET can be obtained from the present equation by letting the elastic anisotropy factor $2(S_{11}-S_{12})/S_{44}=1$. The strain for a given geometry calculated using AET has been compared with the strain calculated using IET by deriving an expression wherein the elastic compliances appear only as the elastic anisotropy factor. In the rest of the article, terms "isotropy" and "anisotropy" will be used to mean, respectively, elastic isotropy and elastic anisotropy.

II. BACKGROUND INFORMATION

A. The diffraction geometries

As the expression for the lattice strain produced by the nonhydrostatic pressure depends on the diffraction geometry of the experiment, we consider in this section the various geometries used in practice. The geometry shown in Fig. 1(a) (termed parallel geometry, PL-G) corresponds to the diamond anvil cell geometry[2] wherein the load direction coincides with direction of the incident x-ray beam. The specimen is a polycrystalline aggregate. It is important to note that all the crystallites in the specimen do not contribute to the diffracted intensity at a given point (the point of observation) on the diffraction ring, but only those whose diffracting-plane normals make an angle $(\pi/2)-\theta$ with the incident x-ray beam [Fig. 1(b)], and lie in the plane containing the incident x-ray beam and the point of observation.

In another geometry [termed perpendicular geometry, PD-G; Fig. 2(a)] the incident x-ray beam is perpendicular to the load direction, and passes through the gap between the anvils.[25–27] This geometry is normally used when the anvil material (e.g., tungsten carbide) is opaque to x rays. The points of observation on the diffraction ring are *A* and *B*, the plane SAB being perpendicular to the load direction. This geometry, although not commonly used now, will be considered for the sake of the completeness of the discussion. Kinsland and Bassett[19,20] used the PD-G with diamond anvils such that the entire diffraction ring, ACBD, could be recorded on a flat film. As discussed later, the lattice strains corresponding to the diffraction ring diameters AB and CD, which are, respectively, perpendicular and parallel to the load direction, are of special interest. The crystallites contributing to the intensities at points A and B are those whose diffracting-plane normals are perpendicular to the load axis and make angles $\pm[(\pi/2)-\theta]$ with the incident x-ray beam [Fig. 2(b)]. The intensities at

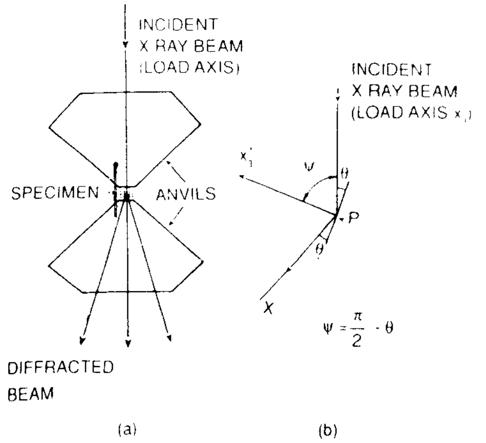

FIG. 1. (a) The parallel geometry (PL-G). (b) *P*-diffracting plane, *x* point of observation; x_3-loading direction, x_3'-diffracting-plane normal.

C and D arise from the crystallites whose diffracting-plane normals make angles $\pm\theta$ with the load direction and lie in the plane SCD [Figs. 2(a) and 2(c)].

The Kinsland–Bassett geometry is of interest as it permits recording in a single exposure of the diffraction data over a large range of ψ values. The method, however, has a drawback in that the incident x-ray beam passes through a region of large pressure differential in the direction of the beam, rendering the data difficult to interpret. This drawback, however, can be overcome by using a beryllium gasket to confine the specimen in a small region around the center of the anvil face.

B. The stress state

The solid specimen flows radially when compressed between the anvils. Under large loads, the specimen surface layers in contact with the anvils remain stationary, and the flow occurs mainly through the shearing of the specimen material.[28] The driving force for the flow arises from the stress gradient and is opposed by the shear strength of the specimen material. As the specimen thickness decreases during the flow, the driving force for the flow also decreases. Soon, equilibrium is reached and the stress field in the specimen during the subsequent x-ray measurements is elastic and independent of time. This stress system will be referred to an orthogonal right-handed co-ordinate system $x_i (i=1,2,3)$ such that the axes x_1 and x_2 are parallel to the anvil face, and the axis x_3 is along the load direction. Let r denote the radial direction in a plane parallel to the anvil face. The origin of the co-ordinate system is chosen at $r=0$ and half way between the two anvil faces. Following the convention used in elasticity theory of single crystals,[29] the stress state at the center of the specimen is given by

$$\sigma_{ij} = \begin{pmatrix} \sigma_1 & 0 & 0 \\ 0 & \sigma_1 & 0 \\ 0 & 0 & \sigma_3 \end{pmatrix}. \tag{1}$$

The difference, $(\sigma_3 - \sigma_1) \equiv t$, was termed uniaxial stress component (USC) in earlier studies.[7,8] The maximum shear or von Mises yield criterion leads to the following relation[17,18]

$$(\sigma_3 - \sigma_1) \equiv t = 2\tau_y = \sigma_y, \tag{2}$$

where τ_y is the shear strength of the specimen material and σ_y the yield strength. The equivalent hydrostatic pressure (mean normal stress) for such a stress system is given by

$$\sigma_p = (\sigma_1 + \sigma_1 + \sigma_3)/3 = (\sigma_1 + t/3). \tag{3}$$

The stress system can also be expressed as the combination of σ_p and the deviatoric stress d_{ij},

$$\sigma_{ij} = \begin{pmatrix} \sigma_p & 0 & 0 \\ 0 & \sigma_p & 0 \\ 0 & 0 & \sigma_p \end{pmatrix} + \begin{pmatrix} -t/3 & 0 & 0 \\ 0 & -t/3 & 0 \\ 0 & 0 & 2t/3 \end{pmatrix}$$

$$= \sigma_p + d_{ij}. \tag{4}$$

In the subsequent discussions the compressive stress and the resulting strain are taken to be negative. Thus, all the compressive stresses have to be taken with a negative sign in all the forthcoming equations.

The flow stress of a material normally depends on the experimental parameters such as the plastic strain rate and strain. The plastic strain rate experienced by the specimen compressed between the anvils is very small as compared with the strain rates encountered during shock compression. Further, the strain rate sensitivity exponent at room temperature is small[30] for most materials. Because of these reasons, the strain rate dependence of flow stress is small. Since the time dependence of strain vanishes soon after the application of the load, even the small flow stress component which may arise from the strain rate relaxes, and t settles at a value slightly below σ_y. The measurements on magnesium oxide[31] show that the yield stress decreases with increasing plastic strain. This trend may be exhibited

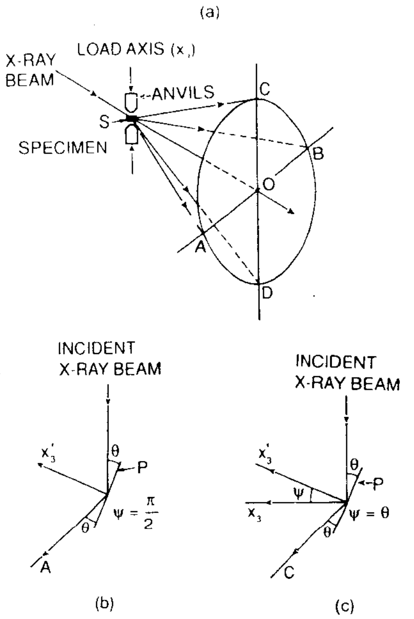

FIG. 2. (a) The perpendicular geometry (PD-G). The diffraction condition for the crystallites contributing to the diffracted intensity (b) at A and (c) at C. The conditions for intensities at B and D are obtained by a 180° rotation of (b) and (c), respectively, about the incident x-ray beam. *P*-diffracting plane, x_3-loading direction, x_3'-diffracting-plane normal.

to ϵ_p produced by σ_p to get the total strain. the quantities t and S_{ij} appearing in the expression for $\epsilon^R(hkl)$ are at pressure σ_p.

B. Iso-strain model (Voigt limit)

The strain ϵ'_{33} under iso-strain (Voigt) model can be calculated by deriving the expression for an elastically isotropic case and substituting for the elastic constants the Voigt average values. The expression for the isotropic case can be obtained by letting $S=0$ in Eq. (16) and noting that $(S_{11}-S_{12})$ equals $(1+\nu)/E$ or $(2G)^{-1}$, where ν, E, and G denote Poisson's ratio, Young's modulus, and shear modulus, respectively. Thus, ϵ'_{33} in the iso-strain model is given by

$$\epsilon'_{33}=\epsilon^V=\epsilon_p+\epsilon_d^V, \tag{17a}$$

where

$$\epsilon_d^V=-\left(\frac{t}{3}\right)(1-3\cos^2\psi)\left(\frac{1+\nu_V}{E_V}\right)$$

$$=-\left(\frac{t}{3}\right)(1-3\cos^2\psi)\left(\frac{1}{2G_V}\right). \tag{17b}$$

The suffix V for the moduli denotes the Voigt average

$$(2G_V)^{-1}=(1+\nu_V)/E_V=\left(\frac{5}{2}\right)\frac{(S_{11}-S_{12})S_{44}}{3(S_{11}-S_{12})+S_{44}}. \tag{18}$$

Since the linear compressibility in both iso-stress and iso-strain models is given by $(S_{11}+2S_{12})$, the expression for ϵ_p remains unchanged, and is given by Eq. (16b). In the numerical estimation of $\epsilon^R(hkl)$ and ϵ^V, σ_p and t are to be used with a negative sign.

C. Measured lattice strains

The lattice strain can be determined from the measured lattice spacing under pressure, using the relation

$$\epsilon_m(hkl)=\frac{[d_{p+d}(hkl)-d_0(hkl)]}{d_0(hkl)}=\frac{[a_{p+d}(hkl)-a_0]}{a_0}, \tag{19}$$

where a denotes the lattice parameter. The suffix $(p+d)$ refers to the nonhydrostatic stress system (σ_p+d_{ij}). If the actual condition lies between those described by iso-stress and iso-strain models, then the measured strain corresponds to the following:

$$\epsilon(hkl)=\epsilon_p+\alpha\epsilon_d^R(hkl)+(1-\alpha)\epsilon_d^V, \tag{20}$$

where α is a fraction and $\epsilon_d^R(hkl)$ and ϵ_d^V are given by Eqs. (16c) and (17b), respectively.

D. Reduced strain equation

In this section the strain equation is expressed in a form which is convenient for quantitatively comparing the present equations with those derived using IET. From Eq. (20) we get

$$\Delta\epsilon(hkl)=\epsilon(hkl)-\epsilon_p=\alpha\epsilon_d^R(hkl)+(1-\alpha)\epsilon_d^V. \tag{21}$$

The specimen is an aggregate of elastically anisotropic crystallites. Let G denote the shear modulus of the bulk solid which is elastically isotropic if a completely random orientation of the crystallites exists. If isotropic elasticity theory is used one gets for this case

$$\Delta\epsilon_{\text{iso}}=-\left(\frac{t}{3}\right)(1-3\cos^2\psi)\left(\frac{1}{2G}\right). \tag{22}$$

The shear modulus of the specimen can be expressed as follows:[40]

$$G=\tfrac{1}{2}(G_R+G_V), \tag{23}$$

where G_R and G_V are the shear moduli under Reuss and Voigt limits, respectively; G_V is given by Eq. (18) and G_R by

$$(2G_R)^{-1}=\tfrac{1}{10}[4(S_{11}-S_{12})+3S_{44}]. \tag{24}$$

The relation given by Eq. (23) is further discussed in the next section. On combining Eqs. (16c), (17b), and (21)-(24) we get

$$R=\frac{\Delta\epsilon(hkl)}{\Delta\epsilon_{\text{iso}}}=\alpha f^R(x,\Gamma)+(1-\alpha)f^V(x), \tag{25}$$

where

$$x=2(S_{11}-S_{12})/S_{44},$$

$$f^R(\Gamma,x)=F_1+F_2,$$

$$F_1=\left(\frac{5}{2}\right)[(1-3\Gamma)x+3\Gamma]\times(3+2x)^{-1},$$

$$F_2=\left(\frac{1}{10x}\right)[(1-3\Gamma)x+3\Gamma]\times(2+3x),$$

and

$$f^V(x)=\tfrac{1}{2}[1+(F_1/F_2)].$$

In practice, the d spacings of a number of reflections are measured, and the reported lattice strains are an average (simple or weighted) over all the measured reflections. In such a case,

$$\langle R\rangle=\alpha\langle f^R(x,\Gamma)\rangle_\Gamma+(1-\alpha)f^V(x). \tag{26}$$

The symbol $\langle\rangle$ denotes the type of average (simple or weighted) used to calculate the average strain from the measured d spacings. The second term is independent of (hkl).

IV. DISCUSSION

A. General

1. Macroscopic and lattice strains

A bulk polycrystalline material consisting of randoml oriented anisotropic crystallites is isotropic. The macr scopic strain in the specimen of such a material, produce by a given stress, can be calculated using IET and th elastic constants of the polycrystalline material. The ma roscopic strain corresponds to the commonly measur strain using a strain gauge or any other macroscopic tec nique. In terms of the elastic constants of the single crystal, the macroscopic strain can be calculated in two ways. In the first procedure, the elastic constants of the polycrystalline material can be calculated by averaging over the orientations of all the crystallites, the single crystal elastic constants under a realistic behavior of the stress and strain across the grain boundaries. The polycrystal elastic constants calculated under the Reuss[35] and Voigt[36] limits represent the lower and upper bounds respectively, and empirically the average of the two is found to be close to the measured value[40] (More refined methods[41–43] narrow the difference between the lower and upper bounds, but the average of the two does not differ appreciably from the average of the Reuss and Voigt values). The macroscopic strain can be calculated using these constants and IET. In the second procedure, the strain can be calculated separately using the two bounds of the elastic constants, and the average of the two strains can be taken to represent the macroscopic strain. It is to be noted that in both procedures the calculation of the macroscopic strain in terms of the single crystal elastic constants requires averaging over the orientations of all the crystallites.

The equivalence of the two procedures depends on the anisotropic factor, x. For an isotropic case ($x=1$) the two procedures are equivalent, and begin to diverge as anisotropy increases, i.e., x deviates from unity. For the range of x values exhibited by the majority of the real materials, the two procedures give strains differing by only a few percent. Equation (20), which gives the lattice strain as the weighted average of the lattice strains calculated under the Reuss and Voigt limits, is obtained following the second procedure. The term, ϵ_d^V, is common to both the calculations of the lattice and macroscopic strains. However, calculations under the Reuss limit differ. The calculation of ϵ_d^R requires an averaging over all possible orientations of the φ groups of crystallites only, whereas the calculation of the macroscopic strain requires an averaging over the orientations of all the crystallites. For this reason the lattice strain, in general, differs from the macroscopic strain in any given direction; this distinction, however, vanishes if the crystallites are isotropic.

2. *The value of* α

The (hkl)-dependence of the lattice strain [Eq. (20)] arises from the term ϵ_d^R. The observation[7–16] of the (hkl) dependence of the measured lattice strains clearly established that $\alpha \neq 0$. The view was expressed[11,20] without any evidence to support it that $\alpha=1$ was relevant to the high pressure measurements. The exact value of α in any experiment has not been estimated so far. The calculations of the polycrystal elastic constants in terms of the single crystal data (discussed in the preceding section) and the strains produced in the polycrystalline specimen by the residual stresses[37] employ the average of the Reuss and Voigt limits. These estimates agree well with the corresponding measured values. If a similar procedure is also employed in the present case, then $\alpha=\frac{1}{2}$.

It may be noted that the value of α is required only for calculating $\Delta\epsilon(hkl)$. Since the compressibilities of a cubic material under Reuss and Voigt limits are the same, α does not appear in the expression for ϵ_p. Even if the compressibilities of the specimen material are different under the two limits as is the case with the polycrystals containing crystallites of lower symmetry, ϵ_p is given by the calculation under the Reuss limit alone. This is supported by a large number of studies on the volume compression of two-phase mixtures (the specimen and the pressure marker), which indicate that the pressures (and not the volume strains) in the two phases are equal.

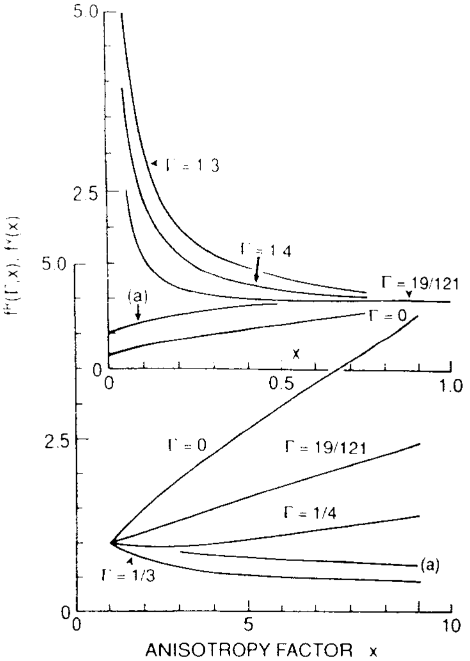

FIG. 4. The $f^R(\Gamma,x)$ vs x plots for different Γ values. $f^V(x)$ vs x plot is marked (a).

B. Estimates of *R* and $\langle R \rangle$

The ratio R as given by Eq. (25) provides a quantitative comparison of the lattice strain (AET) with the macroscopic stain (IET) in the same direction. The $f^R(\Gamma,x)$ vs x plots in the range $0 \leqslant x \leqslant 10$ are shown in Fig. 4 for $\Gamma=0$, $\frac{19}{121}$, $\frac{1}{4}$, and $\frac{1}{3}$. These Γ values pertain to the first five reflections from the face-centered as well as the body-centered cubic structure. The Γ value is zero for 200, $\frac{19}{121}$ for 311, $\frac{1}{4}$ for 110, 220, and 211, and $\frac{1}{3}$ for 111 and 222. The function $f^R(\Gamma,x)$ approaches infinity as x approaches zero for all Γ values, except for zero, for which it is 0.2 at $x=0$. For all values of Γ, the function is unity at $x=1$. With a further increase in x, the function increases and approaches infinity as x approaches infinity for all values of Γ, except for $\frac{1}{3}$ for which it decreases reaching a value of 0.3 at $x=\infty$. The function $f^V(x)$ increases from 0.5 at $x=0$ to 1 at $x=1$, and then decreases slowly reaching 0.5 at $x=\infty$.

The R (with $\alpha=0.5$) vs x plots are shown in Fig. 5. Qualitatively, the plots are similar to those in Fig. 4. The R values are close to unity in the vicinity of $x=1$, and diverge as x either increases or decreases. For a given value of $x(>1)$, the R value decreases with increasing Γ, while the trend is reversed in the region $x<1$. It may be noted that if $\alpha=1$ is assumed then $R=f^R(\Gamma,x)$. The atmospheric

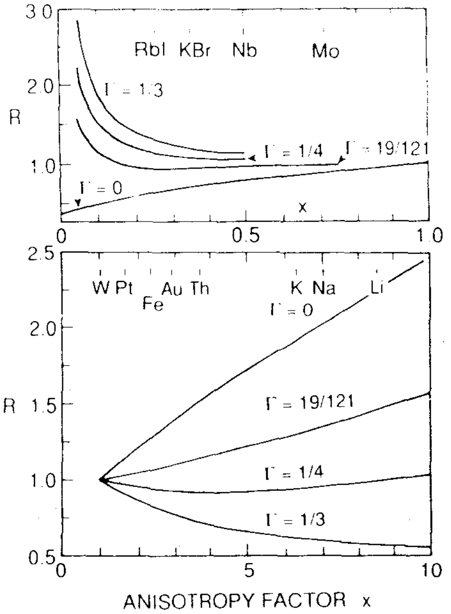

FIG. 5. The R (with $\alpha=0.5$) vs x plots for different Γ values. The atmospheric pressure x values for a few elements are marked.

pressure x values for a few materials are marked on Fig. 5. An examination of the atmospheric pressure elastic data[44] of a large number of elements and compounds indicates that most materials have the x values lying between 0.5 and 4. The alkali metals have unusually large x, whereas the rubidium halides have unusually small x. To illustrate the Γ dependence of R in an actual case, we consider the example of gold ($x\approx 2.9$). The R values are 1.4, 1.1, 0.9, and 0.8 for the Γ values 0, $\frac{19}{121}$, $\frac{1}{4}$, and $\frac{1}{3}$ respectively. It is seen that the R values can differ widely from one reflection to another.

The $\langle R\rangle$ vs x plots for the first three, four, and five reflections from the fcc and bcc structures are shown in Fig. 6. The value of $\langle R\rangle$ for the first five reflections from gold is 1, even though the R values for $\Gamma=0$ and $\frac{1}{3}$ show a large difference. The numerical estimates of R and $\langle R\rangle$ for gold based on the atmospheric pressure x value are valid for the low pressure x-ray diffraction data. The variation of x with pressure should be considered while estimating R and $\langle R\rangle$ in the high pressure region.

C. Various diffraction geometries

1. Perpendicular geometry (PD-G)

The expression for $\epsilon(hkl)$ for PD-G can be obtained by letting $\psi=\pi/2$ in Eq. (20). This gives

$$\begin{aligned}\epsilon(hkl)&=(S_{11}+2S_{12})\sigma_p+(1-\alpha)\epsilon_d^V\\&\quad-\alpha(t/3)(S_{11}-S_{12}-3S\Gamma)\\&=(S_{11}+2S_{12})\sigma_1+(1-\alpha)\epsilon_d^V-\alpha t(S_{12}+S\Gamma).\end{aligned}\tag{27}$$

Equation (27) is the same as Eq. (12) of Singh and Kennedy.[7] It is also clear that the term ϵ_w^p in earlier work[7,8] is the strain produced by the hydrostatic pressure of magnitude σ_1. The $\epsilon(hkl)$ vs $\Gamma(hkl)$ plot is a straight line, the slope m being

$$\begin{aligned}&m=St\alpha,\\&t=(m/\alpha S).\end{aligned}\tag{28}$$

The analysis[11] of the diffraction data assuming $\alpha=1$ on sodium chloride compressed to various pressures up to 10 GPa gave $t=(0.24+0.011p)$ GPa. This suggests that at 9 GPa, $t=0.35$ GPa. The measurement of the pressure gradient[31] in sodium chloride compressed in a diamond anvil cell gave $t=0.54$ GPa at 9 GPa. This value of t can be obtained from the diffraction data[11] if $\alpha=0.65$ is assumed. While making such a comparison, it is to be noted that the value of t may depend on the extent of deformation the specimen undergoes during pressurization.[31]

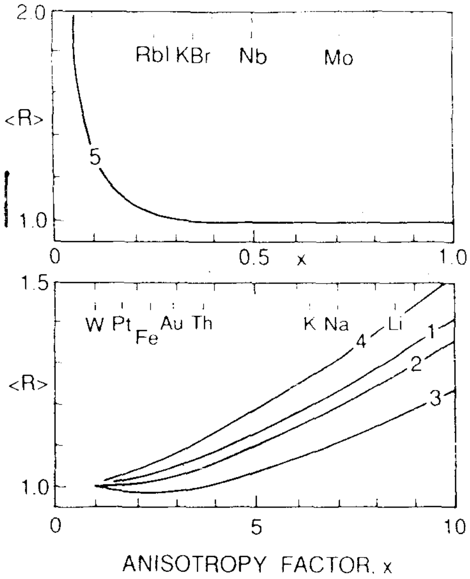

FIG. 6. The $\langle R\rangle$ vs x plots. The average over 1-first three reflections from fcc, 2-first four reflections from fcc, 3-first five reflections from fcc, 4-first three reflections from bcc. The averages over the first four and five reflections from bcc lie close to 2 and 3, respectively. The average over the first three reflections from fcc in the range $0<x\leqslant 1$ is shown by the curve marked 5. Other cases lie close to 5 in the range $0.2\leqslant x\leqslant 1$.

2. Parallel geometry (PL-G)

For the PL-G, $\psi=(\pi/2)-\theta$, and Eq. (20) reduces to

$$\begin{aligned}\epsilon(hkl)&=(S_{11}+2S_{12})\sigma_p+(1-\alpha)\epsilon_d^V\\&\quad-\alpha(t/3)(1-3\sin^2\theta)(S_{11}-S_{12}-3S\Gamma)\\&=(S_{11}+2S_{12})\sigma_1+(1-\alpha)\epsilon_d^V-\alpha t[S_{11}\sin^2\theta\\&\quad+S_{12}\cos^2\theta(1-3\sin^2\theta)S\Gamma].\end{aligned}\tag{30}$$

Equation (30) agrees with the expression derived earlier[8] for PL-G. The σ_1 and t being compressive have to be taken with negative signs. In PL-G, $\epsilon(hkl)$ depends on θ, and therefore, the $\epsilon(hkl)$ vs $\Gamma(hkl)$ plot is not amenable to a simple interpretation as in PD-G. However, the high pressure x-ray diffraction data on sodium chloride have been analyzed[15] with the help of Eq. (30) to obtain meaningful values of the elastic compliance ratios S_{11}/S and $(S_{11}-S_{12})/S$.

In the energy dispersive mode of data collection, θ is a constant, and the $\epsilon(hkl)$ vs $\Gamma(hkl)$ plot is a straight line with the slope

$$m=\alpha tS(1-3\sin^2\theta). \tag{31}$$

Recently, the energy dispersive data from gold in a gold-zirconium mixture[16] were successfully analyzed using a modified form of Eq. (30) and t-values estimated assuming $\alpha=1$.

The expression for an isotropic case can be obtained by letting $S=0$ in Eq. (20), and noting that $(S_{11}-S_{12})=(1+\nu)/E$. It is seen that

$$\epsilon_d^R=\epsilon_d^V=-\left(\frac{t}{3}\right)\left(\frac{1+\nu}{E}\right)(1-3\sin^2\theta). \tag{32}$$

Noting that t is negative, this equation is the same as Eq.(4) derived using IET by Ruoff *et al.*[24] for PL-G.

It is seen from Eqs. (17b) and (29) that the strain produced by the deviatoric stress component vanishes if $\sin\theta=1/\sqrt{3}$, and the measured lattice strain precisely equals ϵ_p. However, because of the various constraints, such high angles are difficult in practice to achieve.

3. *Kinsland–Bassett geometry*

In experiments with the diamond anvil cell in PD-G (Fig. 2), it is observed[19,20] that the x-ray diffraction ring recorded on a flat film placed normal to the incident x-ray beam, it not a circle if the specimen experiences nonhydrostatic pressure. Let the strains calculated from the diffraction ring diameters AB and CD [Fig. 2(a)] be denoted by $\epsilon_\perp$ and ϵ_θ, respectively. As shown in Fig. 2, $\psi=\pi/2$ for observations at A and B, and $\psi=\theta$ for C and D. It can be easily shown using Eq. (20) that

$$(\epsilon_\perp-\epsilon_\theta)=(t\cos^2\theta)[\alpha(S_{11}-S_{12}-3\Gamma S)+(1-\alpha)\times(2G_v)^{-1}]. \tag{33}$$

The corresponding equation in IET ($S=0$) reduces to

$$(\epsilon_\perp-\epsilon_\theta)_{\text{iso}}=(t\cos^2\theta)(2G)^{-1} \tag{34}$$

$$=(t\cos^2\theta)\left(\frac{1+\nu}{1-2\nu}\right)\left(\frac{1}{3B}\right), \tag{35}$$

where B is the bulk modulus. From the measured $(\epsilon_\perp-\epsilon_\theta)$, t can be obtained using Eq. (33) if S_{ij} terms are known as a function of pressure. In the framework of the IET [Eq. (35)], t can be calculated if B and ν as a function of pressure are known. The volume-compression data directly give B as a function of pressure. The pressure dependence of ν is often small and can be ignored. However, it should be kept in mind that the function containing ν in Eq. (35) is quite sensitive to changes in ν.

Kinsland and Bassett[19] determined the strain ellipsoid from the measured ϵ_θ and $\epsilon_\perp$, and calculated $\epsilon_\parallel$, the principal strain along the load direction. It may be noted that $\epsilon_\parallel$ can never be measured in diffraction experiments. Since the calculation of $\epsilon_\parallel$ uses the expression which is valid for macroscopic strains, the expression $(\epsilon_\parallel-\epsilon_\perp)$ using AET will not be discussed. However, if IET is used, then the relevant equation can be obtained by letting $\theta=0$ and $\epsilon_\theta=\epsilon_\parallel$ in Eq. (35). It is not possible to compare either Eq. (33) or (35) with the expressions used by Kinsland and Bassett[20] because the details of the tensor transformation used by them are not given in their paper.

It can be easily shown that the ratio of the strain given by Eq. (33) to the strain given by Eq. (34) equals R. Thus, the error introduced by assuming complete isotropy when the crystallites are actually anisotropic can be estimated from Fig. 5.

V. CONCLUSIONS

(1) The expression for the lattice strain for any geometry used in high pressure x-ray diffraction work can be obtained from the general equation derived in this article, by substituting the appropriate value of ψ (being the angle between the direction of load and the diffracting-plane normal).

(2) The limited data suggest that the average of the strains calculated under the Reuss and Voigt limits represent the true lattice strain arising from the deviatoric stress component. The determination of α using high pressure diffraction data will be of great interest.

(3) The lattice strain corresponds to the stain measured by the x-ray diffraction method. The strain calculated using isotropic elasticity theory gives the macroscopic strain which, in general, differs from the lattice strain. The ratio, R, of the two strains (in the direction of the lattice strain) produced by the deviatoric stress component depends on the elastic anisotropy factor of the crystallites constituting the polycrystalline specimen and the Miller indices (hkl). The two strains are identical only if the crystallites are elastically isotropic.

APPENDIX

The specimen compressed between the anvils undergoes plastic deformation before the static stress field (Sec. II B) is set up. The specimen invariably develops preferred orientation (texture) as a result of the plastic deformation. In such a case, the average values of the geometric functions used in the derivation of Eq. (11) are given by

$$\langle\sin\varphi\rangle=\int_0^{2\pi} n(\varphi)\sin\varphi\, d\varphi \Big/ \int_0^{2\pi} n(\varphi)d\varphi$$

and similar expressions for $\cos\varphi$, $\sin^2\varphi$, and $\cos^2\varphi$. Here, $n(\varphi)$ denotes the number of φ group of crystallites in the range φ and $\varphi+d\varphi$ in the specimen region illuminated by the incident x-ray beam. The term $n(\varphi)$ can be obtained from the crystallite orientation distribution function[45] measured on the specimen recovered after the high pressure experiment.

---

[1] It is possible to produce truly hydrostatic pressure by the use of metal gasket and fluid pressure transmitting medium (for a review of the diamond anvil cell techniques see Ref. 2). The solid specimen is often compressed between the anvils directly either for reaching pressures (see Refs. 3 and 4) near the upper pressure limit or in the experiments

designed for shear strength determination (see Ref. 5).

[2] A. Jayaraman, Rev. Sci. Instrum. **57**, 1013 (1986).

[3] Y. K. Vohra, S. J. Duclos, and A. L. Ruoff, Phys. Rev. B **36**, 9790 (1987).

[4] H. K. Mao, P. M. Bell, K. J. Dunn, R. M. Chrenko, and R. C. DeVries, Rev. Sci. Instrum. **50**, 1002 (1979).

[5] R. Jeanloz, B. K. Godwal, and C. Mead, Nature **349**, 687 (1991).

[6] The term lattice strain refers to the strain calculated from the interplanar spacings measured at high pressure and at one atmosphere by a diffraction method. As discussed later in this article, the lattice strain is not equal to the macroscopic strain in the same direction, if the crystallites of polycrystalline specimen are elastically anisotropic. No such distinction exists if the crystallites are elastically isotropic.

[7] A. K. Singh and G. C. Kennedy, J. Appl. Phys. **45**, 4686 (1974).

[8] A. K. Singh and C. Balasingh, J. Appl. Phys. **48**, 5338 (1977).

[9] A. K. Singh, High Temp-High Pressures **10**, 641 (1978).

[10] J. C. Jamieson (private communication, 1975).

[11] A. K. Singh and G. C. Kennedy, J. Appl. Phys. **47**, 3337 (1976).

[12] K. Syassen and W. B. Holzapfel, Rev. Sci. Instrum. **49**, 1107 (1978).

[13] S. N. Vaidya, W. A. Grosshans, and W. B. Holzapfel, High Temp-High Pressures **16**, 491 (1984).

[14] W. A. Grosshans, E. F. Duesing, and W. B. Holzapfel, High Temp-High Pressures **16**, 539 (1984).

[15] S. Usha Devi and A. K. Singh, Physica B **139–140**, 922 (1986).

[16] A. K. Singh, K. Vijayan, H. Xia, Y. K. Vohra, and A. L. Ruoff, in *Recent Trends in High Pressure Research,* edited by A. K. Singh (Oxford & IBH, New Delhi, 1992), p. 782.

[17] A. L. Ruoff, Scripta Metall. **8**, 1161 (1974).

[18] A. L. Ruoff, J. Appl. Phys. **46**, 1389 (1975).

[19] G. L. Kinsland and W. A. Bassett, Rev. Sci. Instrum. **47**, 130 (1976).

[20] G. L. Kinsland and W. A. Bassett, J. Appl. Phys. **48**, 978 (1977).

[21] G. L. Kinsland, High Temp-High Pressures **10**, 627 (1978).

[22] H. K. Mao, P. M. Bell, J. W. Shaner, and D. J. Steinberg, J. Appl. Phys. **49**, 3276 (1978).

[23] A. L. Ruoff, H. Xia, H. Luo, and Y. K. Vohra, Rev. Sci. Instrum. **61**, 3830 (1990).

[24] A. L. Ruoff, H. Luo, H. Xia, and Y. K. Vohra, High Pressure Res. 6, 183 (1991).

[25] J. C. Jamieson and A. W. Lawson, J. Appl. Phys. **33**, 776 (1962).

[26] E. A. Perez-Albuerne, K. F. Forsgren, and H. G. Drickamer, Rev. Sci. Instrum. **35**, 29 (1964).

[27] D. B. McWhan and W. L. Bond, Rev. Sci. Instrum. **35**, 626 (1964).

[28] N. H. Polakowski and E. J. Ripling, *Strnegth and Structure of Engineering Materials* (Prentice Hall, Englewood Cliffs, NJ, 1966), pp. 302-309.

[29] J. F. Nye, *Physical Properties of Crystals* (Oxford University, London, 1960).

[30] P. Van Houtte, in *Numerical Modelling of Material Deformation Processes,* edited by P. Hartley, I. Pillinger, and C. E. N. Sturgess (Springer, London, 1992), p. 95.

[31] C. Mead and R. Jeanloz, J. Geo. Phys. Res. **93**, 3261 (1988).

[32] A. K. Singh, in *Recent Trends in High Pressure Research,* edited by A. K. Singh (Oxford & IBH, New Delhi, 1992), p. 786.

[33] C.-M. Sung, C. Goetze, and H.-K. Mao, Rev. Sci. Instrum. **48**, 1386 (1977).

[34] H. Kimura, D. G. Ast, and W. A. Basset, J. Appl. Phys. **53**, 3523 (1982).

[35] A. Reuss and Z. Angew, Math. Mech. **9**, 49 (1929).

[36] W. Voigt, *Lehrbuch der Kristalphysik* (Teubner, Liepzig, 1928).

[37] G. B. Greenough, in *Progress in Metal Physics,* edited by B. Chalmers (Pergamon, New York, 1952), Vol. 3, p. 176.

[38] E. Macherauch and U. Wolfstieg, Mater. Sci. Eng. **30**, 1 (1977).

[39] I. C. Noyan and J. B. Cohen, *Residual Stress: Meaurement by Diffraction and Interpretation* (Springer, New York, 1987).

[40] R. Hill, Proc. Phys. Soc. (London) A **65**, 349 (1952).

[41] E. Kroner, Z. Physik **151**, 504 (1958).

[42] Z. Hashin and S. Shtrikman, J. Mech. Phys. Solids **10**, 335 (1962).

[43] Z. Hashin and S. Shtrikman, J. Mech. Phys. Solids **10**, 343 (1962).

[44] G. Simmons and H. Wang, *Single Crystal Elastic Constants and Calculated Aggregate Properties: A Handbook* (M.I.T., Cambridge, MA, 1971).

[45] H. J. Bunge, *Texture Analysis in Materials Science* (Butterworths, London, 1982).